SiGe-based Reconfigurable Current Sensor for Lunar Applications

Obadiah Kegege, Matt Barlow, Alan Mantooth
University of Arkansas
Fayetteville, Arkansas 72701, USA
okegege@uark.edu, mbarlow@uark.edu, mantooth@uark.edu

Abstract - *A reconfigurable four-channel current sensor for cryogenic space applications was implemented. Actuators for space applications range from instrument positioning to motors for driving rovers, and in-situ drilling equipment (~ 100mA to about 10A). A current sensor capable of operation in cryogenic temperatures is required to protect equipment being operated in space missions. The components of this current sensor are: a flash Analog-to-Digital Converter (ADC), encoder, constant current source/mirror, and 4-channel analog multiplexer. This sensor will measure current going to four different power stages through a 0.02 Ω sense resistor. The sensor will: (i) provide two scales of current sensing within 0A to 15 A that would work with a variety of spacecraft instruments as well as in-situ exploration rovers, (ii) operate within -180 ˚C to 125 ˚C, (iii) ensure low power consumption and optimum modes of control/operation, and (iv) enable reconfigurability for high resolution at the scale of mA.*

Keywords: Current sensor, Flash ADC, SiGe Electronics, Cryogenics, Lunar electronic.

1 Introduction

A reconfigurable current sensor with a wide measurement scale for lunar applications was implemented using a flash ADC, encoder, constant current source/mirror, and 4-channel analog multiplexer. This sensor was designed in commercially available radiation hardened Silicon-Germanium (SiGe) BiCMOS technology. The temperature on lunar surface ranges from -180 ˚C to +125 ˚C, and -230 ˚C inside shadowed polar craters. Also, there are radiation effects such as single event upset (SEU), solar events, and total ionizing dose (TID). For lunar surface exploration, electronics and systems must be able to withstand thermal cycling and 100 krad of radiation over 10 years. SiGe electronics have tested to operate down to -230 ˚C (43 K) [1]. And, several papers have been published demonstrating the radiation hardness and operational capabilities of SiGe devices for cryogenic space missions/lunar applications [2-5].

A common technique for design of ADCs is to use comparators. A 4-bit ADC uses 15 comparators, 5-bit uses 31comparators, 6-bit uses 63 comparators, and the trend keeps on increasing by 2^n -1 comparators, where n = number of bits. The higher the number of comparators and resistors, the higher the resolution, and more power is consumed. A 4-bit flash ADC can be applicable in a system where the desired speed is high and a relatively low resolution would provide reliable data. Design techniques have been used to optimize a 4-bit flash ADC to act as a virtual 5-bit ADC to achieve a wide range and high resolution of current measurement. The optimized 4-bit flash ADC architecture and other components integrated in the design of this reconfigurable current sensor are analyzed in the following sections.

2 Current Sensor Design Overview

2.1 Low Power Flash ADC Architecture

A typical n-bit flash ADC is designed using 2^n -1 comparators, a resistor bank to provide a reference voltage for each comparator (2^n -1 stepping levels), and an encoder to change the output code to binary code. However, other methods exist for designing ADCs. The resolution of the ADC is determined from the number of comparators and the choice of the resistor bank. As shown in Figure 1, the (quantization step) for the ADC is given by Equation 1.

$$\Delta_{Vref} = \frac{V_{\mathrm{Re}f(+)} - V_{\mathrm{Re}f(-)}}{2^n - 1} \quad (1)$$

and

$$V_{Ri} = V_{R(i-1)} + \Delta_{Vref} \quad (2)$$

where i = 1, 2, 3 ….. 2^n -1.

As the ADC input signal (V_in) increases, a comparator would produce a high voltage logic level (3.3V) if it were greater or equal to its reference voltage. The increase is linear producing a code that increases like a thermometer as the comparators turn on, from Comp_1 to Comp_(2^n -1), as shown in Figure 1. This code is then fed into the n-bit encoder that changes it to binary code.

Using Ohms law, we find that the voltage drop when 15A flows across a 0.02 Ω sense resistor is 300mV (Table 1). To design a current sensor that can measure up to 15A using a linear 5-bit ADC, we have: Δ_{Vref} = 300/31 = 9.7 mV. So, the smallest measured current step is 0.0097V / 0.02Ω = 484 mA.

Table 1. Design Parameters for ADC Design – Virtual 5-bit.

Sense Resistor (Ω)	Current Flow Lower Scale (A)	Comp. Vref (mV) Ic = 10μA	Current Flow Upper Scale (A)	Comp. Vref (mV) Ic = 100μA	Ref. Resistor #	Resistor Bank (Ω)
0.02	0	0	0	0	0	0
0.02	0.1	2	1	20	R1	200
0.02	0.2	4	2	40	R2	400
0.02	0.3	6	3	60	R3	600
0.02	0.4	8	4	80	R4	800
0.02	0.5	10	5	100	R5	1000
0.02	0.6	12	6	120	R6	1200
0.02	0.7	14	7	140	R7	1400
0.02	0.8	16	8	160	R8	1600
0.02	0.9	18	9	180	R9	1800
0.02	1	20	10	200	R10	2000
0.02	1.1	22	11	220	R11	2200
0.02	1.2	24	12	240	R12	2400
0.02	1.3	26	13	260	R13	2600
0.02	1.4	28	14	280	R14	2800
0.02	1.5	30	15	300	R15	3000

Then $A_{R1,R2,R3,\ldots,R(2n-1)}$ = 484 mA, 968 mA, 1452 mA, …, 15A. This will result in only two quantization steps within the mA scale (as demonstrated later in Figure 3).

The block diagram of ADC is included in Figure 1. The input "Sleep" is an active low signal to turn off the dc biasing of the circuit to achieve low power dissipation when not needed. The input common mode down to 0V eliminates the need to use an amplifier to increase the voltage output of the current sense resistor.

The optimum resolution (enhanced Δ_{Vref}) and low power have been achieved by using a 4-bit ADC and reconfiguring the reference voltage of the comparator bank. The "CONFIG_CURR" input shown in Figure 2 controls the configuration of this reference voltage. When CONFIG_CURR = 1, we have 10 μA flowing through the resistor bank, and when CONFIG_CURR = 0, we have 100μA flowing through the resistor bank. This results in lesser components and higher precision in the mA scale as compared to using a 5-bit ADC and a linear scale. The calculations for the two measurement scales are shown in Table 1. The lower scale covers 0mA to 1500mA, whereas the upper scale covers 0A to 15A. There is slight overlap at the edge between the two scales for redundancy.

The ADC comparator bank is designed using a low power continuous time comparator [6] with the following parameters: output swing of 0 – 3.3V, average power consumption of 130 μW, input common mode range of 0V to 2.4V, and V_{bias} required is 1.15 V. This comparator was fabricated and tested to reliably operate within the temperature range of –180 °C to 125 °C.

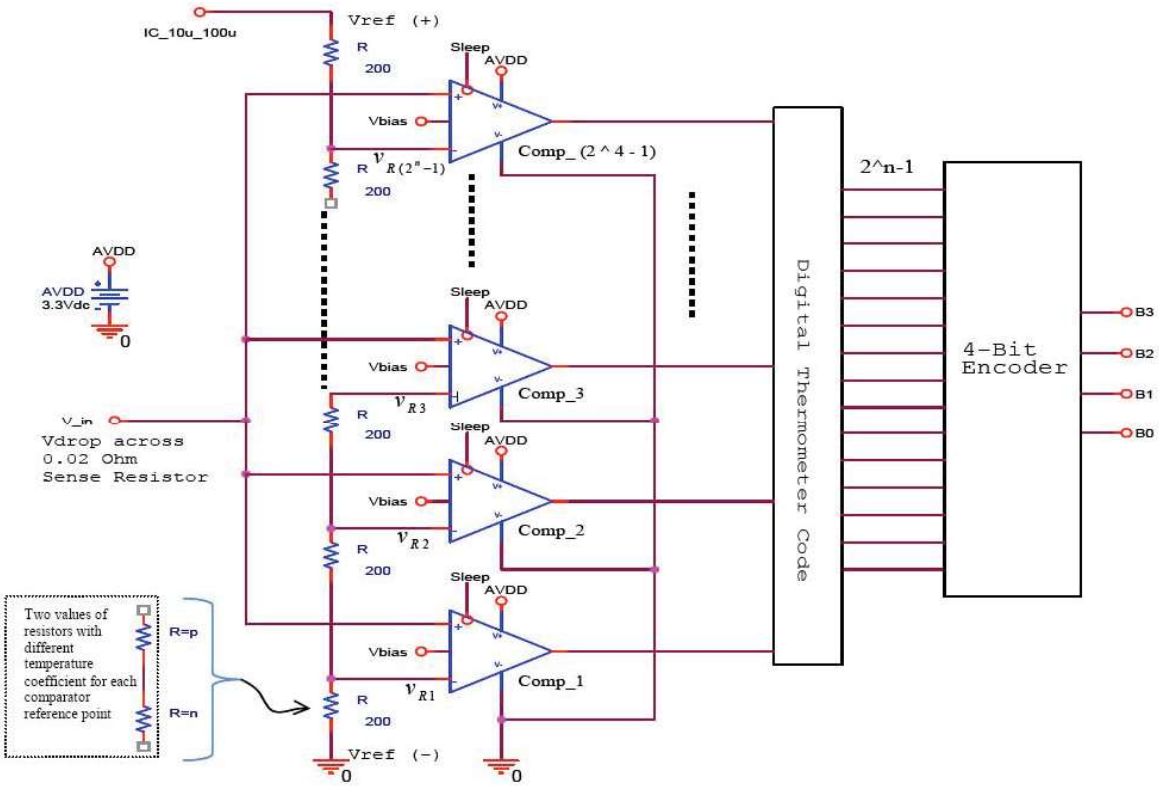

Figure 1. 4-bit flash ADC architecture.

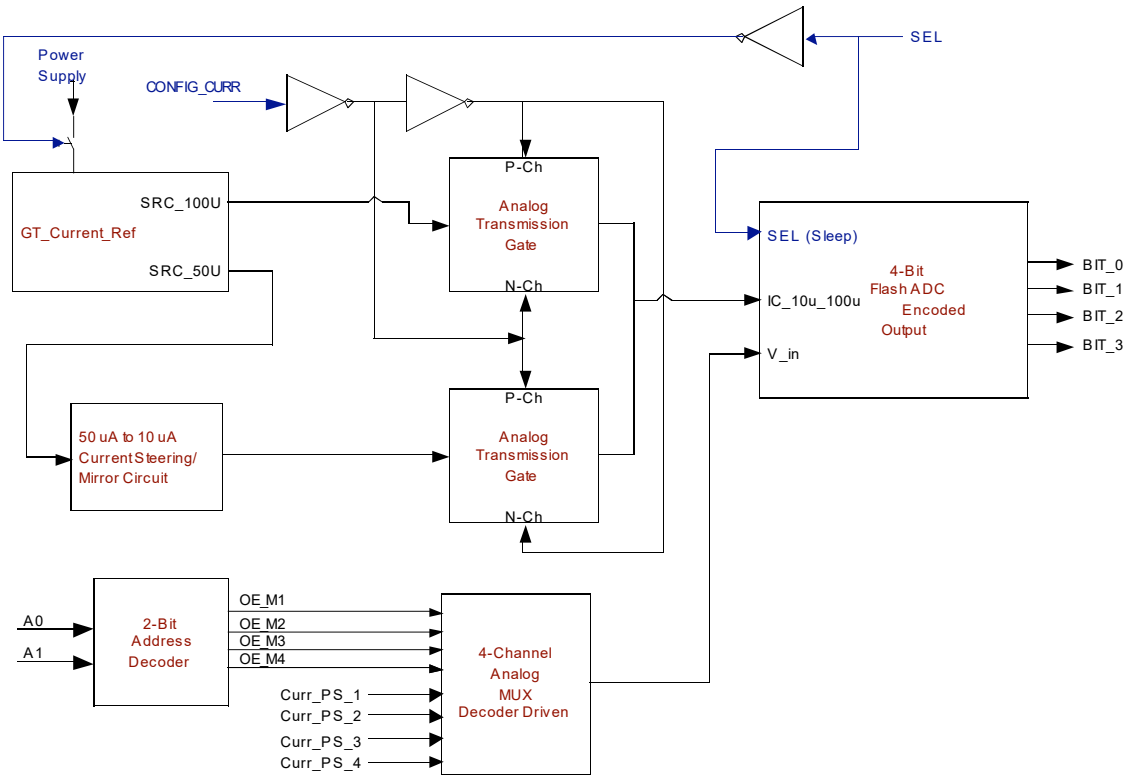

Figure 2. Four-channel reconfigurable current sensor block diagram.

The proposed measurement scales are shown in Figure 3. Since this is a microcontroller based current sensor, start-up defaults on the lower mA scale. In an event where current reaches 1500mA, the microcontroller configures the ADC reference to the upper scale.

The actual measurement scenario using this optimized design with less components/lower power sensor is demonstrated in Figure 4.

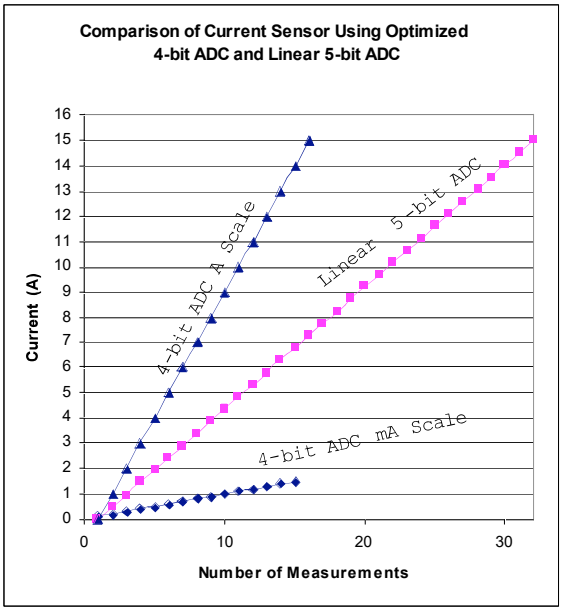

Figure 3. Two scales of measurement obtained by an optimized virtual 5-bit ADC.

Actual measurement scenario

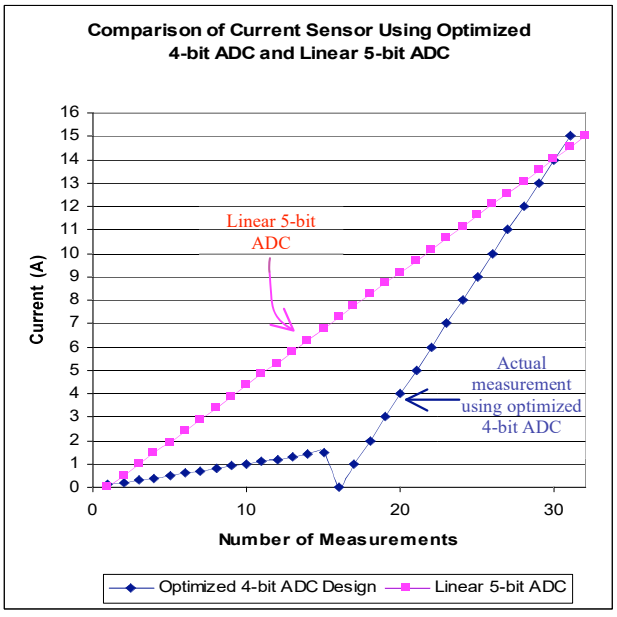

Figure 4. Current sensing using optimized virtual 5-bit ADC.

2.2 Four-Channel Reconfigurable Current Sensor

The block diagram of the integrated current sensor is shown in Figure 2, and the layout in Figure 5. The address decoder (A0, A1) selects the channel to measure. Analog transmission gates switch the selected current for configuring the reference voltage. "SEL" input sets the "Sleep" high or low. The ADC takes most of the area in the layout and also consumes more power as compared to other circuits in the same layout. The other modules in this layout are: the encoder, constant current source, current steering circuit/mirror, and 4-channel analog multiplexer.

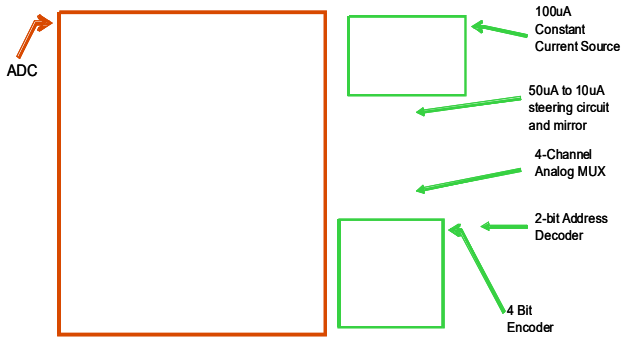

Figure 5. Layout for the four-channel reconfigurable current sensor.

3 Simulation Results and Analysis

In Figure 6 is the current sensor output when a 80 ns current spike of 0–15 A (Tr = 50ns, Tf = 20ns, PW = 10ns) is measured, testing sensitivity and full range of the current sensor. This simulation was repeated for the temperatures between 180 ˚C to 125 ˚C at intervals of 10 ˚C.

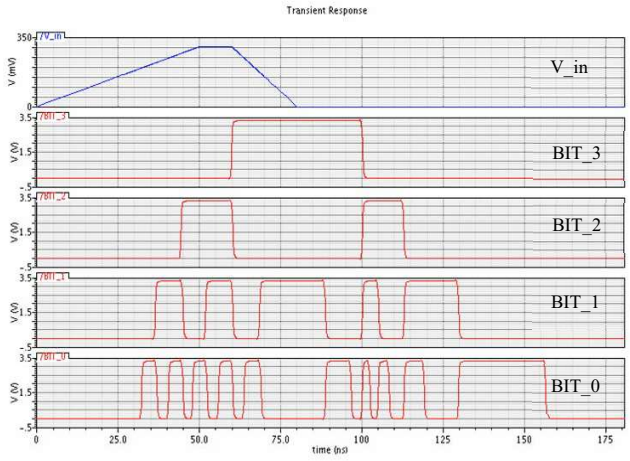

Figure 6. A simulated 80 ns current spike at -180 ˚C.

Each of the four channels confirmed similar results. As shown in Figures 6, BIT_0, BIT_1, BIT_2, and BIT_3 are the data outputs from the current sensor to the microcontroller. There is a propagation delay of 32 ns. Also, the binary output starting with lower bit (BIT_0) to high bit (BIT_3) is confirmed for the rise time and fall times.

Also, other simulations were done to test operation of the lower and upper measurement scales within the full temperature range (Figure 7). In this simulation, a 1.55 A pulse (PW=4 µs) is measured in the lower scale first (CONFIG_CURR = 1), then switched to the upper scale (CONFIG_CURR = 0). This pulse has a 31 mV drop across the 0.02 Ω sense resistor.

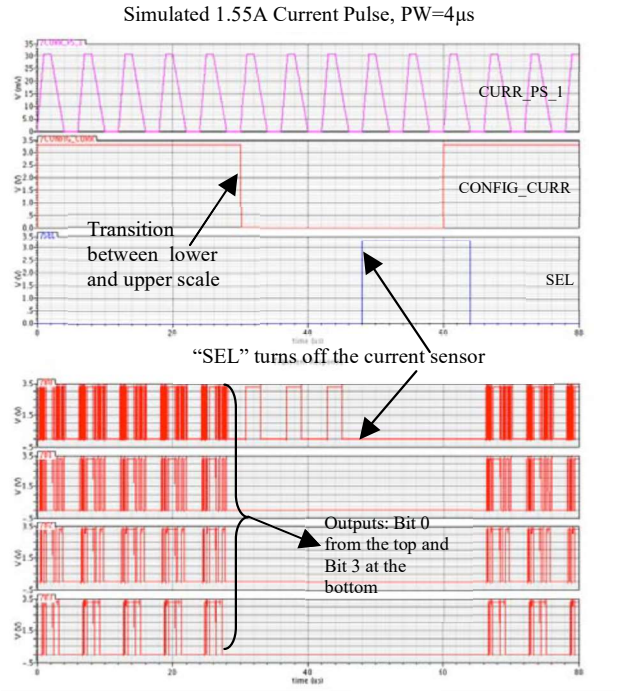

Figure 7. A simulated current of 1.55 A at -180 ˚C.

As seen in Figure 7, when the microcontroller switches to upper scale (CONFIG_CURR = 0), the sensor only outputs Bit 0 of the upper scale, instead of full range in the lower scale. The voltage drop has to be up to 40 mV for the next quantization level in the upper scale (refer to Table 1 and Figure 3).

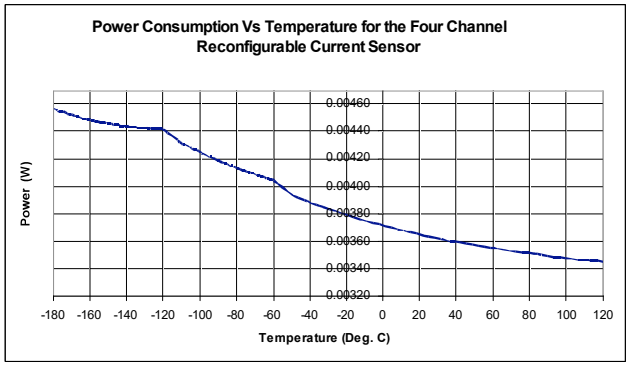

Figure 8. Power consumption vs. temperature for reconfigurable current sensor.

As seen from Figure 8, the propagation delay and power consumption increases with the decrease in temperature. Other simulated parameters are shown in Table 2.

Table 2. Simulated parameters for current sensor.

Parameters	Min	Max	Units
Power Consumption	3.5	4.6	mW
Propagation delay	32	51	ns
Frequency Range	x	12	MHz
Layout Area	1600 * 1380		μ M

4 Conclusions

A four-channel reconfigurable current sensor was designed and modeled for stability throughout -180 ˚C to 125 ˚C. This paper covered the design, modeling, simulations, and Cadence layout only. The chip will be fabricated in commercially available radiation hardened Silicon-Germanium (SiGe) BiCMOS technology and get tested after fabrication. Past and current space missions i.e. Mars Science Laboratory (MSL) rover to be launched in December 2011 use/have used radiation shielding, both active and passive thermal control mechanisms to keep electronic components and other space systems within their operating temperature ranges [7, 8]. These mechanisms include insulation, warm boxes, heat sinks/radiators, and mechanically pumped fluid loops (MPFL). Thermal control mechanisms increase weight, volume, system power drain, launch costs, and the use warm boxes dictates centralized wirings architectures (the use of long cables that can negatively impact safety and reliability).

This wide range current sensor that can withstand thermal cycling and radiation on the Moon will measure 0 – 15 A at a high resolution than a linear 5-bit ADC based current sensor. It achieves low power (a maximum of 4.6 mW) by using the same resistor bank and a 4-bit ADC (but a virtual 5-bit) for two scales of measurement. Another advantage, it achieves 30 quantization levels with a 4-bit ADC: 15 quantization levels between 0 – 1500 mA and 15 quantization levels for upper range between 0 – 15 A, with slight overlap at the edge for redundancy. These particular design techniques have not been used before.

On the surface of Mars, it is not that critical for SiGe based electronics when we consider a temperature swing of -90 ˚C to +20 ˚C (night to day). This reconfigurable current sensor will be applicable to both Lunar and Mars: rovers, robotics, in-situ sampling instrumentation, life support systems, and spacecraft instrument positioning systems. If required that a high resolution ADC be used for other similar measurements, the detailed optimization design techniques can still be applied to obtain a wide measurement scale.

Acknowledgment

Authors would like to acknowledge the support from SiGe electronics partners in other universities and industry: IBM, Boeing, BAE Systems, Lynguent, Georgia Institute of Technology, NASA/Jet Propulsion Laboratory, University of Tennessee, Auburn University, University of Maryland, and Vanderbilt University.

References

[1] J. Yuan, J.D. Cressler, Y. Cui, et al, “On the profile design of SiGe HBTs for RF lunar applications down to 43 K,” Proc. 2008 IEEE Bipolar/BiCMOS Circuits and Technology Meeting, Monterey, CA, pp. 25-28, Oct. 2008.

[2] A.S. Keys, J.H. Adams, J.D. Cressler, et al, “High-performance, radiation-hardened electronics for space and lunar environments,” Proc. Space Technology and Applications International Forum, Albuquerque, NM, Vol. 969, pp. 749-756, 2008.

[3] J.D. Cressler, “SiGe BiCMOS technology: An IC design platform for extreme environment electronics applications,” Proc. 45th IEEE International Reliability Physics Symposium, Phoenix, AZ, pp. 141-149, Apr. 2007.

[4] P. Cheng, B. Jun, A. Sutton, et al., “Probing radiation- and hot electron-induced damage processes in SiGe HBTs using mixed-mode electrical stress,” Proc. IEEE Nuclear and Space Radiation Effects Conference, Honolulu, HI, Vol. 54, July 2007.

[5] R.R. Ward, W.J. Dawson, L. Zhu, et al., “SiGe semiconductor devices for cryogenic power electronics – IV,” Proc. 21st IEEE Applied Power Electronics Conference and Exposition, Dallas, TX, Mar. 2006.

[6] R. Broughton, K. Cornett, J. Vandersand, et al, “SiGe BiCMOS low power voltage comparator for extreme temperature range applications”, *International Journal of Highly Reliable Electronic Systems Design,* pp. 13-19, 2008.

[7] P. Bhandari, G. Birur, M. Pauken, et al., “Mars Science Laboratory thermal control architecture,” *Transactions of SAE International*, Vol. 114, No. 1, pp. 130-137, 2005.

[8] G. Birur, P. Bhandari, M. Prina, et al., “Mechanically pumped fluid loop technologies for thermal control of future mars rovers,” Proc. International Conference On Environmental Systems, Norfolk, VA, Paper 2006-01-2035, July 2006.